Eur. Phys. J. D **43**, 225–228 (2007)
DOI: 10.1140/epjd/e2007-00098-4

THE EUROPEAN PHYSICAL JOURNAL D

Magnetism in artificial lattices

K. Kärkkäinen[1,a], M. Borgh[1], M. Manninen[2], and S.M. Reimann[1]

[1] Mathematical Physics, LTH, Lund University, 22100 Lund, Sweden
[2] NanoScience Center, Department of Physics, 40351 University of Jyväkylä, Finland

Received 24 July 2006 / Received in final form 18 October 2006
Published online 24 May 2007

Abstract. We compare magnetism in two artificial lattice structures, a quantum dot array formed in a two-dimensional electron gas and an optical lattice loaded with repulsive, contact-interacting fermionic atoms. When the tunneling between the lattice sites is strong, both lattices are non-magnetic. With reduced tunneling in the tight-binding limit, the shell-filling of the single-site quantum wells combined with Hund's rule determines the magnetism. This leads to a systematic magnetic phase diagram with non-magnetic, ferromagnetic and antiferromagnetic phases.

PACS. 75.75.+a Magnetic properties of nanostructures – 03.75.Ss Degenerate Fermi gases

1 Introduction

Artificially confined quantum systems have proved to be a basis for future nanotechnological applications. One has been able to confine a small number of conduction electrons of a two-dimensional electron gas formed in a layered semiconductor heterostructure by using etching and gating techniques. Experiments and electronic structure calculations have shown that the external confinement gives rise to a quantum-mechanical shell structure [1]. Occupation of shells leads to characteristic features in the addition spectrum and total spin. Single quantum dots can be coupled electrostatically to form artificial molecules and lattices. In contrast to real solids where the atomic bonding defines the band structure, the inter-dot coupling is tunable in quantum dot lattices, which allows for constructing artificial lattices with designed band structures.

More recently, degenerate atomic quantum gases confined into optical and magnetic traps have drawn growing interest after the celebrated discovery of Bose-Einstein condensation [2,3]. Ultra-cold atom gases have opened an exciting laboratory to explore many-particle systems that are not accessible in conventional atomic or solid state physics. As another advance, ultra-cold atoms can be trapped into an optical lattice created by standing laser waves [4–6]. They provide a unique setup to study artificial crystal structures with tunable physical parameters. The physical properties of optically trapped quantum gases and electrons in solids are closely linked. Optical lattices, however, are free of defects and allow for studies of more coherent structures contrary to their solid-state counterparts. An optical lattice is a periodic array of microscopic quantum wells, each confining a small number of atoms. The confined atoms can have several hyperfine states from which a smaller set can be selected. The tunneling and the localization of atoms in the lattice are controlled by the lattice depth which can be tuned by changing the laser intensity. This allows for a smooth transition from a tightly bound lattice to a system of nearly free atoms. The main interaction mechanism in a weakly interacting, dilute atom gas is the s-wave scattering. The strength of this short-range contact interaction can be tuned in the vicinity of a Feshbach resonance [7].

In a bosonic optical lattice, the Mott insulator-superfluid quantum phase transition is realized [8,9]. Fermionic atoms in a three-dimensional lattice were experimentally studied by Köhl et al. [10]. Experiments show that a gradual filling of the lattice transforms the system from a normal state into a band insulator. In addition, by using the Feshbach resonance, a dynamically induced transition between lowest Bloch bands is achieved. The transition is revealed by probing the Fermi surface through absorption imaging [10].

2 Magnetism in artificial lattices

In condensed matter physics, magnetic correlations are attributed to the alignment of electron spins. The Hubbard model provides a simple Hamiltonian that is widely used to describe magnetism in solids and nanostructures [11,12]. It has also been argued that the Hubbard model is well-suited for describing atom dynamics in an optical lattice [8]. In experiments, the hopping parameter can be adjusted with the potential depth and the local interactions are described by the on-site interaction parameter.

[a] e-mail: kimmo.karkkainen@matfys.lth.se

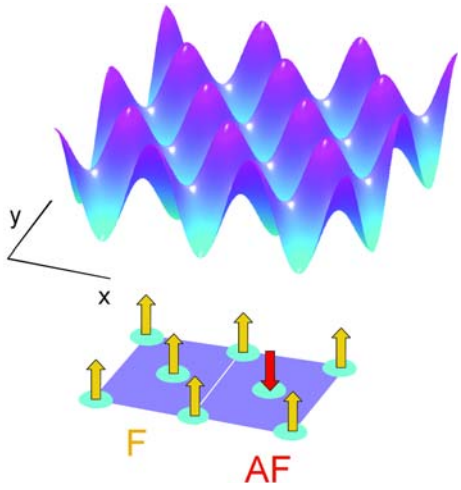

Fig. 1. (Color online) A two-dimensional sinusoidal optical lattice potential. Below is a schematic picture of the square lattice with the unit cell containing two lattice sites allowing for antiferromagnetic (AF) and ferromagnetic (F) orderings of single-site spins.

The Hubbard model assumes the lowest band approximation, allowing at most two atoms per lattice site. In our study, we apply a mean-field approach to explore two-dimensional square lattices formed by quantum dots, or interfering laser beams. The lattice and unit cell is shown schematically in Figure 1. There are two lattice sites per unit cell for the magnetism to be observed. Hund's rule and the single-site shell structure play a central role in determining the magnetic properties of quantum dot lattices confining long-range interacting electrons [13] and optical lattices with short-range contact-interacting fermionic atoms.

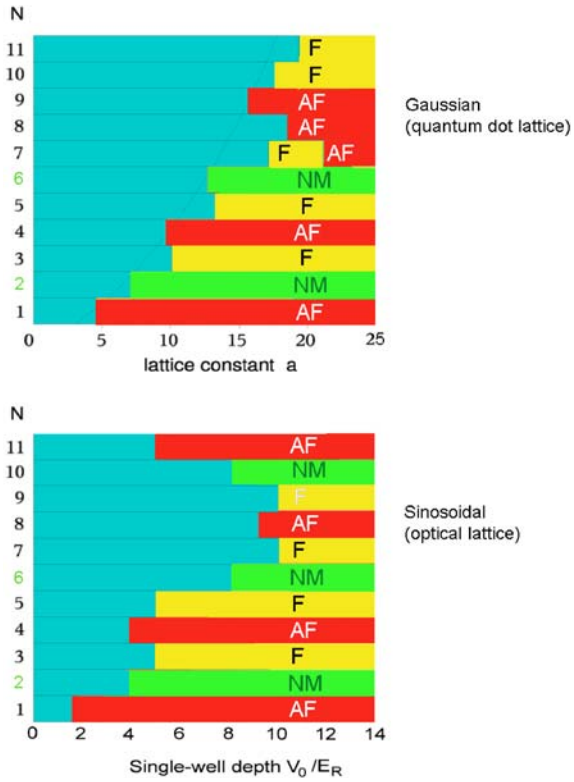

Fig. 2. (Color online) Upper panel: magnetism in a square lattice of quantum dots with $N \leq 11$ electrons per dot, as a function of the lattice constant a (in atomic units). Lower panel: magnetism in sinusoidal optical lattice with fermionic atoms, as a function of lattice depth V_0. The gapless (metallic) phase is blue and the color-coded magnetic phases are antiferromagnetic (AF, red), ferromagnetic (F, yellow) and non-magnetic (NM, green).

2.1 Quantum dot lattice

Magnetism in a two-dimensional square lattice formed by electrostatically coupled quantum dots was earlier investigated in reference [14]. In contrast to the sinusoidal optical lattice displayed above, which experimentally can be created by crossed lasers, the confinement for the electrons was provided by a commensurate positive background charge distribution in order to ensure over all charge neutrality. The background distribution consists of a sum of Gaussians centered at the desired lattice sites. The bottom of the confinement potential at each site is nearly parabolic giving rise to closed shell configurations at electron numbers $N = 2, 6$ and 12 per lattice site. These "magic" numbers are non-magnetic with spin $S = 0$. The orbital degeneracy at mid shell leads to maximization of spin at $N = 4$ ($S = 1$) and 9 ($S = 3/2$) in accordance with Hund's first rule.

Spin-density functional formalism in the local density approximation was used to calculate the ground state for interacting electrons moving in the (quasi-)two-dimensional plane. Due to the periodic boundary conditions, the Kohn-Sham orbitals are of Bloch form. The states and the band energies are labeled by the band index n, wave vector $\mathbf{k}$ and spin $\sigma = (\uparrow, \downarrow)$.

A magnetic phase diagram of the square quantum dot lattice as a function of the number of electrons per single dot N and the lattice constant a is shown in the upper part of Figure 2. The non-magnetic, gapless (metallic) phase is indicated with blue. Spin alignment is indicated by colors and abbreviations. The magnetism sets on at increasingly larger lattice constants as the spatial extent of the highest occupied orbital increases with N. At larger values of a, the individual dots are more isolated and the electrons become tightly bound to the lattice sites. In this limit, the spin is determined by the occupancy of the energy levels at the single quantum dots. We note that at closed shells $N = 2, 6$ and 12 (corresponding to shell closures of $1s$, $1p$ and $2s1d$-shells, respectively) the lattice is non-magnetic. At mid-shell, for $N = 1, 4$ and 9, the band is exactly half-filled. In this situation, the lattice lowers its energy by opening a gap at the Fermi-surface. The gap results from the spin-Peierls transition associated with the antiferromagnetic spin ordering. At open shells the Fermi-level resides in a band, and therefore, the lattices tend to be ferromagnetic metals.

2.2 Optical lattice

We note that fabricating a lattice consisting of identical solid-state quantum dots is not easy. The shell structures of the individual dots should be rather similar for the magnetic effects to appear. Almost perfect square lattices can be created with interfering lasers that provide confinement for fermionic atoms. We found that the shell effects can lead to magnetic phenomena also in optical lattices loaded with weakly interacting, repulsive fermions. We consider fermionic atoms with two hyperfine species confined into a two-dimensional optical lattice. In the contact-interacting two-component fermion gas there is no interaction between same species atom due to the Pauli exclusion principle. Therefore, the trapped atoms occupying a degenerate shell can lower their interaction energy by maximizing the number of atoms of the same species or, in other words, by aligning their spins. This mechanism leads to Hund's rules and magnetism, in close similarity to Coulomb interacting electrons in quantum dot lattices. Here, Hund's rule has a more dramatic effect as it removes completely the interaction between the same-species atoms.

An optical lattice is created by counter-propagating laser beams. The resulting potential, a sinusoidal standing wave $V_{opt}(\mathbf{r}) = V_0(\cos^2(kx) + \cos^2(ky))$, is depicted in the upper panel of Figure 1. The amplitude V_0 is proportional to the laser intensity and wave number $k = 2\pi/\lambda$ is set by the laser wave length [4–6]. A natural unit for the energy is the recoil energy $E_R = \hbar^2 k^2/(2m)$. The standing waves form a square lattice from which we choose a unit cell containing two lattice sites. The inter-site tunneling can be tuned by varying the lattice depth V_0. With increasing V_0 the atoms become more localized at the lattice sites, the band dispersion decreases and the shells in the individual traps are separated by increasingly large gaps.

The ground state of the dilute fermion atom gas is solved from Kohn-Sham-like equations where the exact exchange potential is local. The periodic Bloch functions $u_{n\mathbf{k}\sigma}(\mathbf{r})$ satisfy equations

$$-\frac{\hbar^2}{2m}(\nabla + i\mathbf{k})^2 u_{n\mathbf{k}\sigma}(\mathbf{r}) + (V_{opt}(\mathbf{r}) + g n^{\sigma'}(\mathbf{r}))u_{n\mathbf{k}\sigma}(\mathbf{r}) = \varepsilon_{n\mathbf{k}\sigma} u_{n\mathbf{k}\sigma}(\mathbf{r}), \quad \sigma \neq \sigma' \quad (1)$$

where m is the atom mass, n^σ is the density of atom species σ and g is the interaction strength which we have fixed to $g = 0.3E_R/k^2$. The periodic functions are expanded in plane wave basis and for the Bloch wave vector $\mathbf{k}$ a grid of 5×5 up to 9×9 is used. The self-consistent iterations are started with antiferromagnetic and ferromagnetic initial potentials.

The lower part of Figure 2 shows the magnetism in an optical lattice with N fermionic atoms per lattice site, as a function of the depth of the lattice V_0. The magnetic phases set on in deeper lattices when the atom wave functions are localized at the lattice sites and the spin per site is determined by the occupancy of the single-site energy levels. The bottom of a single-site potential can be approximated by a harmonic potential with $\hbar\omega = \sqrt{4V_0E_R}$.

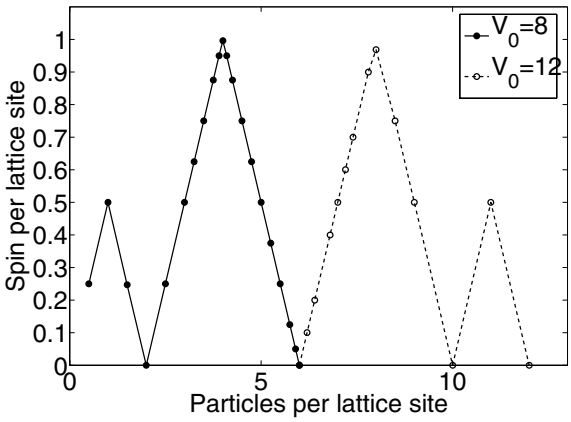

Fig. 3. Integrated spin $S/\hbar$ in a single optical lattice site as a function of particle number N. The depth of lattice is fixed at $V_0 = 8E_R$ for atom number $N \leq 6$ (solid line) and $V_0 = 12E_R$ for $N \geq 6$ (dotted line). The spin and, thus, magnetism follows the shell occupancy of the single quantum wells at lattice sites.

At higher energies, the potential has a square symmetry due to a notch connecting the different lattice sites. It breaks the three-fold orbital degeneracy of the $2s1d$ oscillator shell. Therefore, the closed shells correspond to atom numbers $N = 2, 6, 10$ and 12 per lattice site. These cases are non-magnetic with spin $S = 0$. For $N = 1, 4, 8$ and 11 the valence shells of the single traps are half-filled. Due to Hund's first rule, the orbital degeneracy is resolved by maximizing the spin per lattice site. For these atom numbers, the Fermi-level resides exactly in the middle of the band and the energy is lowered by opening a gap at the Fermi-level. This is due to the spin-Peierls effect of antiferromagnetic spin ordering. For other atom numbers the shell is only partially filled and the Fermi-level resides in a band resulting in a ferromagnetic lattice.

Figure 3 shows spin per lattice site as a function of atom number N. The spin per lattice site is obtained by integrating the spin density over a single lattice site,

$$S = \frac{\hbar}{2}\int_{site} \left[n^\uparrow(\mathbf{r}) - n^\downarrow(\mathbf{r})\right] d\mathbf{r}. \quad (2)$$

In order to be in the tightly-bound limit, where the magnetism sets on, the depth of the lattice is fixed to $V_0 = 8E_R$ for atom numbers $N =$ 1–6 (corresponding to $1s$ and $1p$ shells) and $V_0 = 12E_R$ for $N =$ 7–12 in the $2s1s$ shell. The spin maximization at half-filled shell for atom numbers $N = 1, 4, 8$ and 11 can be seen. The spin and magnetism vanish at closed shell configurations $N = 2, 6, 10$ and 12. We notice that the integrated spin per site develops linearly with particle number.

The detection of magnetic phases in ultracold Fermigases has been discussed in in reference [15] where spin-selective Bragg spectroscopy is proposed to detect long-range antiferromagnetic order. The use of quantum noise interferometry has also been proposed [16].

3 Summary

We found that artificial lattices exhibit intriguing magnetic effects in close similarity to solid state magnetism. The occupancy of the single lattice site quantum wells and Hund's rule determine the magnetic phases in the semiconductor quantum dot lattices and optical lattice with fermionic atoms. The fermionic optical lattices could, therefore, serve to test the current theories of magnetism in a defect-free environment. Hund's rule applies to contact-interacting atoms in a dramatic manner, removing completely the interaction between like atoms. This leads to antiferromagnetism when the single-site valence shell is half-occupied. At closed shells spins are compensated and no magnetism is observed. For other atom numbers, both the lattices tend to favor ferromagnetism.

This study was financially supported by the swedish research council, the swedish foundation for strategic reseach, the finnish academy of science, and the european community project ULTRA-1D (NMP4-CT-2003-505457).

References

1. S.M. Reimann, M. Manninen, Rev. Mod. Phys. **74**, 1283 (2002)
2. M.H. Anderson, J.R. Ensher, M.R. Matthews, C.E. Wieman, E.A. Cornell, Science **269**, 198 (1995)
3. K.B. Davis, M.-O. Mewes, M.R. Andrews, N.J. van Druten, D.S. Durfee, D.M. Kurn, W. Ketterle, Phys. Rev. Lett. **75**, 3969 (1995)
4. P. Verkerk, B. Lounis, C. Salomon, C. Cohen-Tannoudji, J.-Y. Courtois, G. Grynberg, Phys. Rev. Lett. **68**, 3861 (1992)
5. G. Raithel, G. Birkl, A. Kastberg, W.D. Phillips, S.L. Rolston, Phys. Rev. Lett. **78**, 630 (1997)
6. G. Modugno, F. Ferlaino, R. Heidemann, G. Roati, M. Inguscio, Phys. Rev. A **68**, 011601(R) (2003)
7. H. Feshbach, Ann. Phys. **5**, 337 (1958)
8. D. Jaksch, C. Brunder, J.I. Cirac, C.W. Gardiner, P. Zoller, Phys. Rev. Lett. **81**, 3108 (1998)
9. M. Greiner, O. Mandel, T. Esslinger, T.W. Hänsch, I. Bloch, Nature **415**, 39 (2002)
10. M. Köhl, H. Moritz,T. Stöferle, K. Günter, T. Esslinger, Phys. Rev. Lett. **94**, 080403 (2005)
11. J. Hubbard, Proc. R. Soc. Lond. A **276**, 238 (1963)
12. S. Viefers, P. Koskinen, P. Singha Deo, M. Manninen, Physica E **21**, 1 (2004)
13. J. Kolehmainen, S.M. Reimann, M. Koskinen, M. Manninen, Eur. Phys. J. B **13**, 731 (2000)
14. M. Koskinen, S.M. Reimann, M. Manninen, Phys. Rev. Lett. **90**, 066802 (2003)
15. F. Werner, O. Parcollet, A. Georges, S.R. Hassan, Phys. Rev. Lett. **95**, 056401 (2005)
16. E. Altman, E. Delmer, M.D. Lukin, Phys. Rev. A **70**, 013603 (2004)